materials

MDPI

Article

Topological Phase and Strong Correlation in Rare-Earth Hexaborides XB_6 (X = La, Ce, Pr, Nd, Pm, Sm, Eu)

Sheng-Hsiung Hung [1] and Horng-Tay Jeng [1,2,3,*]

[1] Department of Physics, National Tsing Hua University, Hsinchu 30013, Taiwan; feynman0121@gmail.com
[2] Physics Division, National Center for Theoretical Sciences, Hsinchu 30013, Taiwan
[3] Institute of Physics, Academia Sinica, Taipei 11529, Taiwan
* Correspondence: jeng@phys.nthu.edu.tw

Received: 27 August 2020; Accepted: 28 September 2020; Published: 1 October 2020

Abstract: The rare-earth hexaboride SmB_6, known as the topological Kondo insulator, has attracted tremendous attention in recent years. It was revealed that the topological phase of SmB_6 is insensitive to the value of on-site Coulomb interactions (Hubbard U), indicating that the topological phase in SmB_6 is robust against strong correlations. On the contrary, the isostructural YbB_6 displays a sensitivity to the Hubbard U value. As U increases, YbB_6 transforms from topological Kondo insulator to trivial insulator, showing the weak robustness of the topological phase of YbB_6 against U. Consequently, the dependence of the topological phase on Hubbard U is a crucial issue in the rare-earth hexaboride family. In this work, we investigate the structural and electronic properties of rare-earth hexaboride compounds through first-principles calculations based on density functional theory. By taking the strong correlations into consideration using a wide range of on-site U values, we study the evolution of the topological phases in rare-earth hexaboride (XB_6, X = La, Ce, Pr, Nd, Pm, Sm, Eu). Unlike YbB_6, the topological trends in all the examples of XB_6 studied in this work are insensitive to the U values. We conclude that in addition to the well-known SmB_6, PmB_6, NdB_6 and EuB_6 are also topologically nontrivial compounds, whereas LaB_6, CeB_6 and PrB_6 are topologically trivial metal.

Keywords: topological phase; strong correlation; Hexaboride; first-principles calculations; electronic structures

1. Introduction

The discovery of the topological phase in condensed matter paved the way to classify electronic states [1,2]. Topological insulators have been attracting world-wide extensive attention in recent research [3–6]. Three dimensional materials with time reversal symmetry and inversion symmetry may harbor a topologically nontrivial phase if a band gap and band inversion emerge owing to spin–orbit interaction (SOI) [7].

The rare earth hexaboride XB_6 crystallizes in the CaB_6-structure, as shown in Figure 1. Its lattice structure is similar to a body-centered cubic such as the CsCl-type lattice with Cs replaced by rare earth ions, and with Cl substituted by B_6 octahedra. The variety of the physical properties observed in these compounds is intriguing. For example, the application of LaB_6 has been paid attention due to its low work function, which is suitable for thermionic emission. LaB_6 is metallic and becomes superconducting at T_C = 0.45 K [8]. CeB_6 is considered as a Kondo system. CeB_6 presents an antiferro-quadrupolar ordering in the paramagnetic phase between T_q = 3.3 K (quadrupolar ordering temperature) and T_N = 2.4 K (Neel's Temperature) [9,10]. PrB_6 has been confirmed that negative quadrupolar pair interactions exist in the paramagnetic phase (T_N = 6.9 K) [11]. NdB_6 is a localized 4f

system that orders ferro-magnetically at low temperatures [12]. SmB_6 is a well-known topological Kondo insulator [1,13,14]. EuB_6 orders ferro-magnetically below 15.1 K with a huge decrease of resistivity and a significant blue shift of the reflectivity plasma edge [15–17]. At 12.7 K, another phase transition takes place, which is observed as a broad peak in the specific heat or an anomaly in the resistivity [18]. GdB_6 is a localized 4f system with a ferromagnetic order at low temperatures [19]. YbB_6 is a topology Kondo insulator at low temperatures, and is a classical mixed valence narrow band gap semiconductor [1,20,21]. Structural studies are also presented in Ref. [22,23]. As reported in Ref. [1], the topological phase of YbB_6 is sensitive to the Hubbard U value. As U increases, YbB_6 transforms from topological Kondo insulator to trivial insulator, showing the weak robustness of the topological phase of YbB_6 against U.

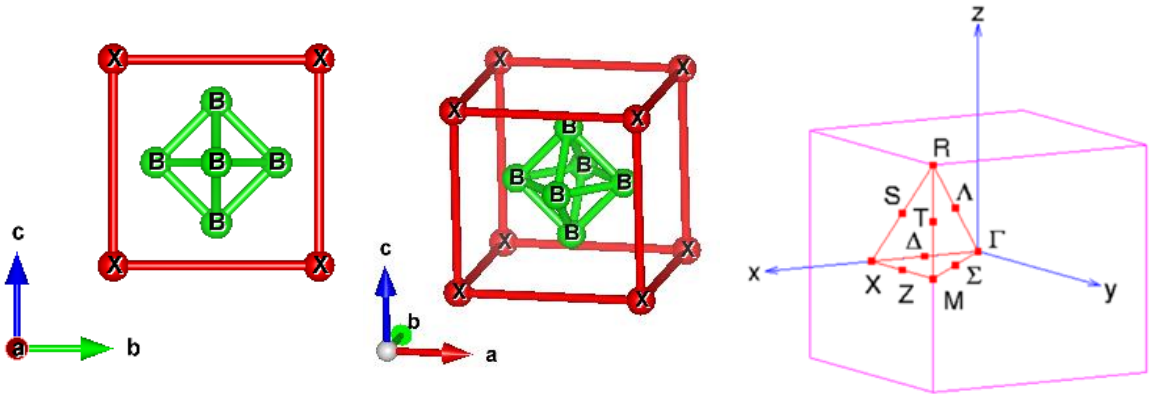

(**a**) (**b**) (**c**)

Figure 1. CsCl-type cubic crystal structure and Brillouin Zone of rare-earth hexaboride XB_6. (**a**) Side view. (**b**) Oblique view. (**c**) Brillouin Zone and high symmetry k-points.

In this study, the lattice structures of rare-earth hexaboride (XB_6, X = La, Ce, Pr, Nd, Pm, Sm, Eu) are fully optimized through first-principles calculations. We then perform self-consistent field electronic structure calculations with and without SOI. To reveal the topological phases, we analyze if SOI would open up a continuous energy gap at the Fermi level with band inversion around the energy gap. To examine the robustness of the topological phase upon the strong correlation in XB_6, we trace the evolution of its electronic structure by tuning the on-site U of the f electrons. We demonstrate that besides SmB_6, PmB_6, NdB_6 and EuB_6 are also topologically nontrivial compounds, while the others are topologically trivial normal metals.

2. Computational Details

First-principles calculations were performed using the Vienna Ab initio Simulation Package (VASP) with the Perdew-Burke-Ernzerhof (PBE) exchange-correlation functional used in the generalized gradient approximation (GGA) as well as the GGA plus Hubbard U (GGA + U) schemes [24–27] based on density functional theory (DFT). The cut-off energy of 500 eV was adopted for the plane-wave basis. A Γ-centered 15 × 15 × 15 k-mesh was used in geometry optimization and self-consistent field calculations. The geometry optimization converged until all residual forces remained below 0.01 eV/Å. Table 1 compares the experimental lattice parameters of rare-earth hexaboride with our geometrically optimized ones. Good agreement between experimental and theoretical results can be found with deviations, in general, of less than 1%.

Table 1. Experimental (exp) and theoretical (the) lattice parameters. The rare-earth hexaboride crystalizes in a bcc-like structure with space group of $Pm\bar{3}m$ (No. 221), in which metal ions are located at the Wyckoff position 1a(0,0,0) and octahedral B_6 at the Wyckoff position 6f (1/2,1/2,z). The subscripts "exp" and "the" indicate experimental and theoretical results, respectively.

	a_{exp} (Å)	a_{the}(Å)	Error of a	$B(z)_{exp}$	$B(z)_{the}$	B–B Bond $Length_{exp}$(Å)	B–B Bond $Length_{the}$(Å)
LaB_6 [15]	4.1527	4.1553	0.06%	0.1993	0.1997	1.7660	1.7647
CeB_6 [16]	4.14	4.1130	−0.65%	0.1992	0.1984	1.7611	1.7543
PrB_6 [22]	4.13	4.1024	−0.67%	0.2	0.1984	1.7522	1.7498
NdB_6 [16]	4.127	4.1007	−0.64%	0.1989	0.1987	1.7574	1.7473
PmB_6 [23]	4.128	4.1131	−0.36%	0.2	0.1990	1.7514	1.7508
SmB_6 [28]	4.1346	4.1087	−0.63%	0.2018	0.1993	1.7436	1.7474
EuB_6 [29]	4.1849	4.1325	−1.25%	0.2027	0.1999	1.7595	1.7539
YbB_6 [29]	4.1444	4.1325	−0.29%	0.207	0.2007	1.7173	1.7492

3. Results and Discussion

3.1. Topologically Trivial Normal Metal LaB_6, CeB_6, and PrB_6

Figure 2a,b show the PBE band structures of LaB_6 without and with SOI, respectively. The atom-orbital decomposition demonstrates that the valence bands below −1.5 eV are mainly composed of B-p orbital, while the conduction La-f bands (blue curves) are located mainly from 0.5 eV to 2.5 eV above the Fermi level (E_f). In between, there is a dispersive band composed of La-d orbital connecting the valence and conduction bands, resulting in an overall semimetal character. This in-gap La-d band also gives an electron pocket at E_f along ΓM. A comparison of band structures without SOI (a) and with SOI (b) shows that the SOI in LaB_6 is weak and has no significant effect on band structure. Consequently, the semimetal character remains as SOI is included. Without any continuous gap, LaB_6 is therefore a topologically trivial normal metal. On the other hand, the band structures remain more or less the same when the on-site Coulomb repulsion U is taken into account for the strong correlation in f orbitals, as can be seen in Figure 3. This constitutes preassembly, owing to the empty f states that have no effect near E_f.

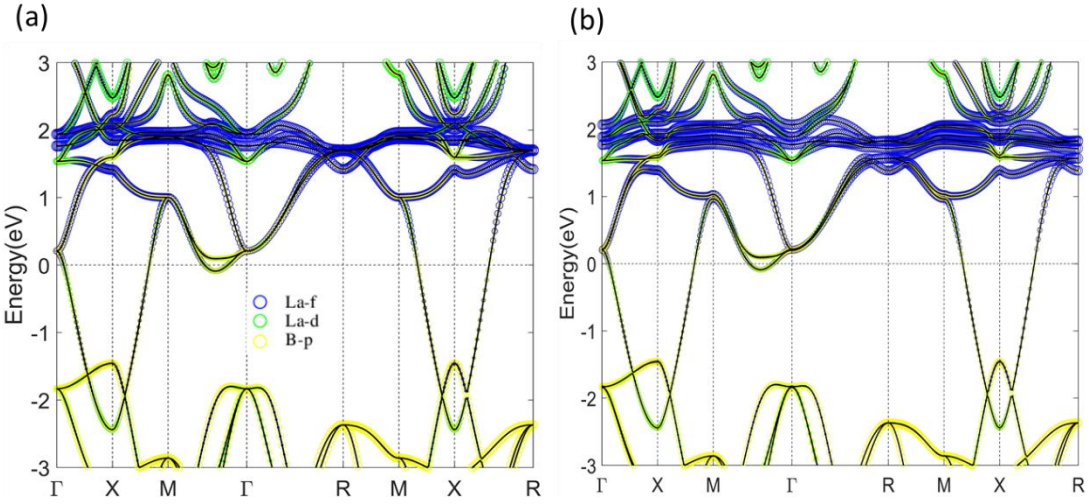

Figure 2. Atom-orbital decomposed band structure of LaB_6 calculated using Perdew–Burke–Ernzerhof (PBE) functional without spin–orbit interaction (SOI) (**a**) and with SOI (**b**). The size of blue, green and yellow circles indicates components from La-f, La-d and B-p orbitals, respectively.

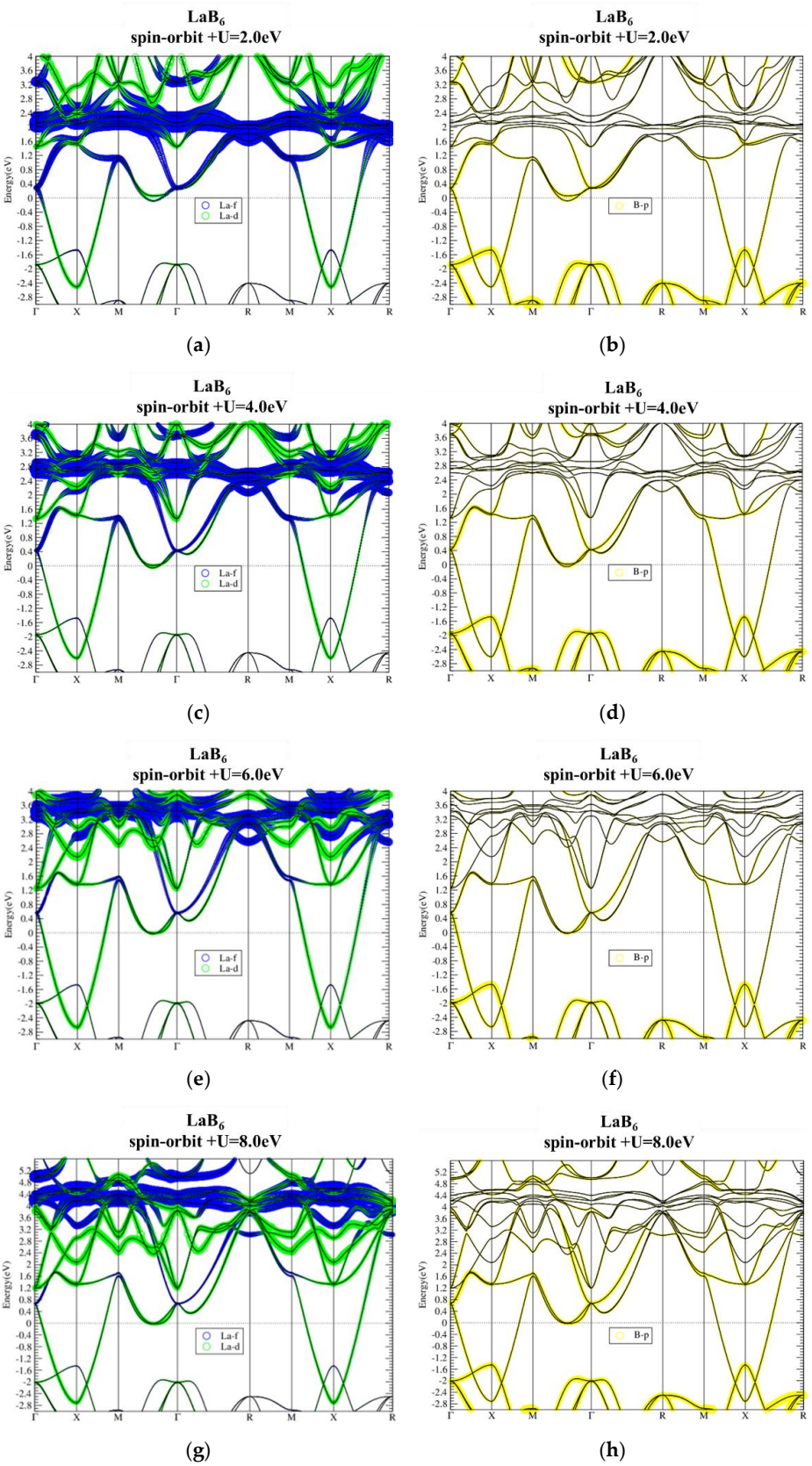

Figure 3. Atom-orbital decomposed band structures of LaB_6 with on-site U =2 eV (**a**,**b**), 4 eV (**c**,**d**), 6 eV (**e**,**f**), and 8 eV (**g**,**h**).

With one more electron than La, the Fermi level of CeB_6 is thus raised up to the bottom of Ce-f bands, as shown in Figure 4. The flat Ce-f conduction bands are located around E_f from 0.6 eV below to 1.2 eV above E_f. As shown in Figure 5, for all the four cases with U = 2, 4, 6, 8 eV studied, there are no significant changes in band structures. Similar to LaB_6, CeB_6 is also insensitive to the on-site U values. Although the SOI is included in the calculations and the degeneracy at M is lifted by SOI, there is no continuous gap in all cases, leading to topologically trivial normal metal ground state for CeB_6.

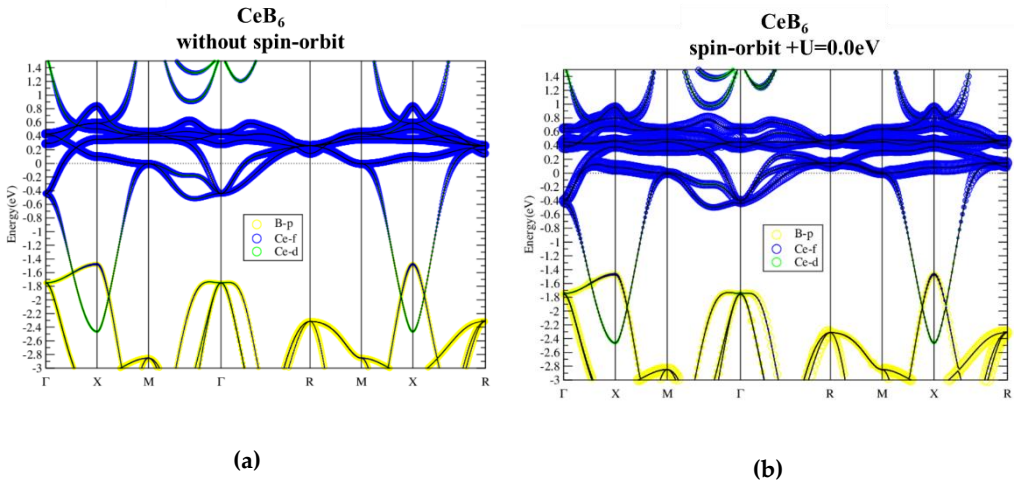

Figure 4. Band structure of CeB_6 without (**a**) and with (**b**) spin–orbit interaction.

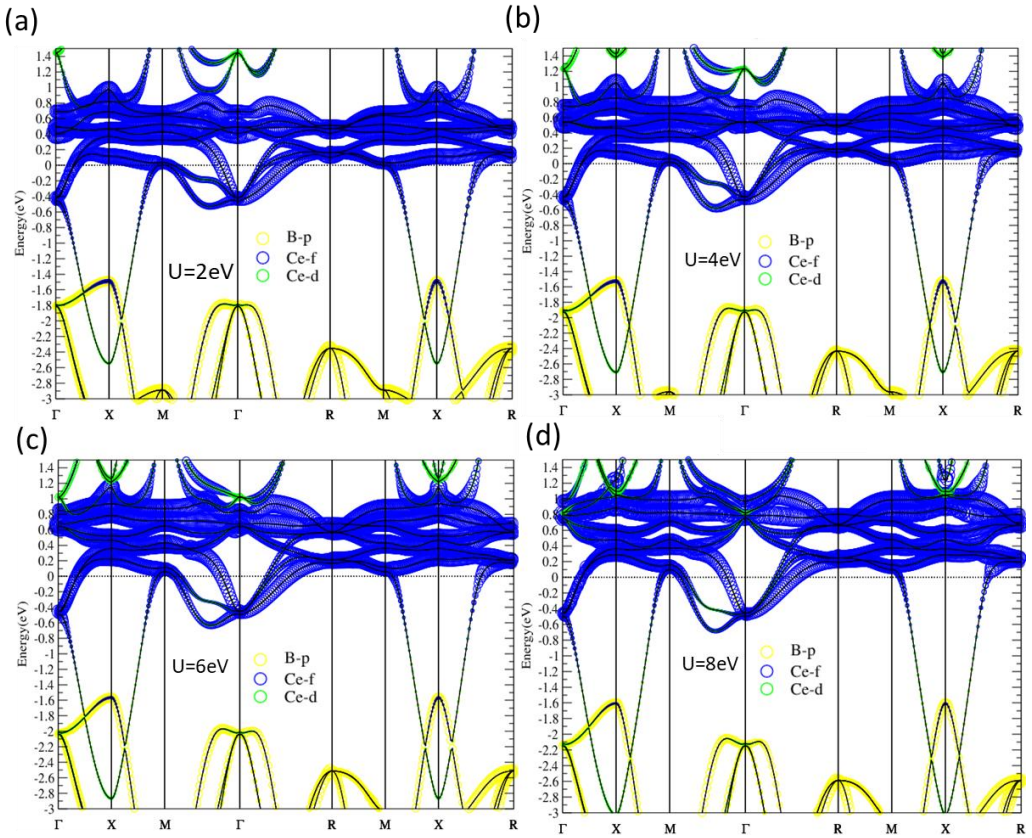

Figure 5. (**a**–**d**) CeB_6 band structures given from PBE + SOI + U with U = 2, 4, 6, 8 eV, respectively. The sizes of blue, green and yellow circles indicate components from Ce-f, Ce-d and B-p orbitals, respectively.

Elementary Pr has three electrons occupying the f-orbitals in the ground state. Therefore, in PrB_6 the Pr-f conduction band is occupied by one more f electron than CeB_6 through the rigid-band shift, as shown in Figure 6. The band dispersions remain similar with different on-site U values. However, because the Fermi level is raised to the middle of the Pr-f conduction band, on-site U affects the bandwidth more significantly than that in the previous two species. With U = 8.0 eV, the f bandwidth is enhanced by about 0.5 eV. On the other hand, gapless ground state remains in PrB_6 even when the SOI is taken into consideration. Consequently, the same as LaB_6 and CeB_6, PrB_6 is also a topologically trivial normal metal.

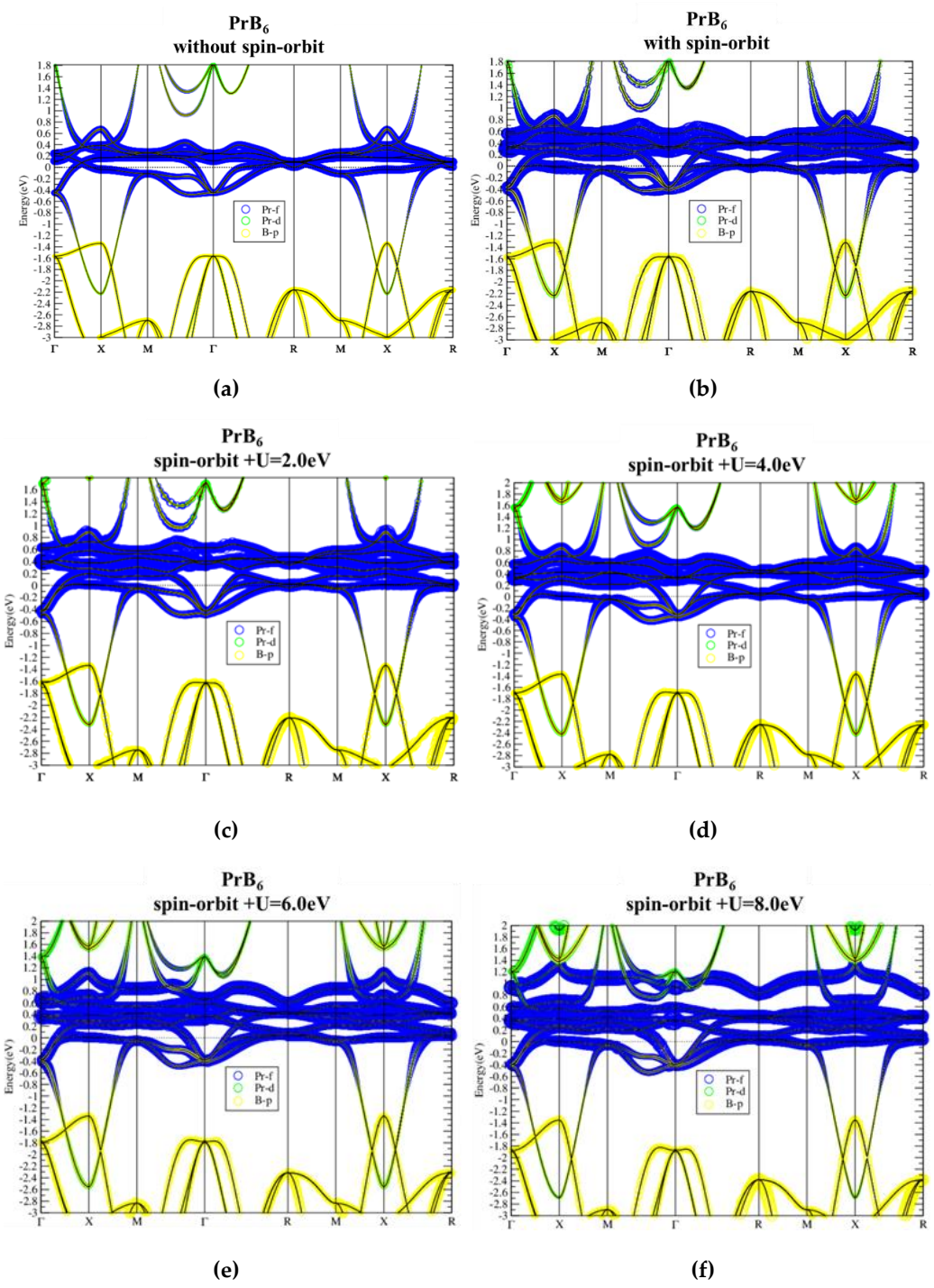

Figure 6. PrB_6 band structure without (**a**) and with (**b**) spin–orbit interaction (noted in the figures), and with spin–orbit interaction plus on-site U = 2, 4, 6, 8 eV (**c**–**f**, respectively) as noted in the figures.

3.2. Topologically Nontrivial Kondo Insulator SmB_6, PmB_6, NdB_6 and EuB_6

Figure 7 shows our calculated band structures of the well-known topological Kondo insulator. The relatively flat La-f bands locate around Ef, with a much more dispersive La-d band crossing all these f bands. The spin–orbit interaction splits the f bands and opens up a continuous energy gap (see Figure 8) with band inversion between Sm-f/d characters flipping around the SOI-induced gap. These results agree well with those presented in previous works [1]. Band structures of SmB_6 with SOI and on-site U ranging from 2 to 8 eV are shown in Figure 9. There are no significant changes in band structures due to all the different U values used. Similar to previous study, the SOI-induced band gap and the band inversion behavior remain, indicating the robust topological phase against strong correlations in SmB_6.

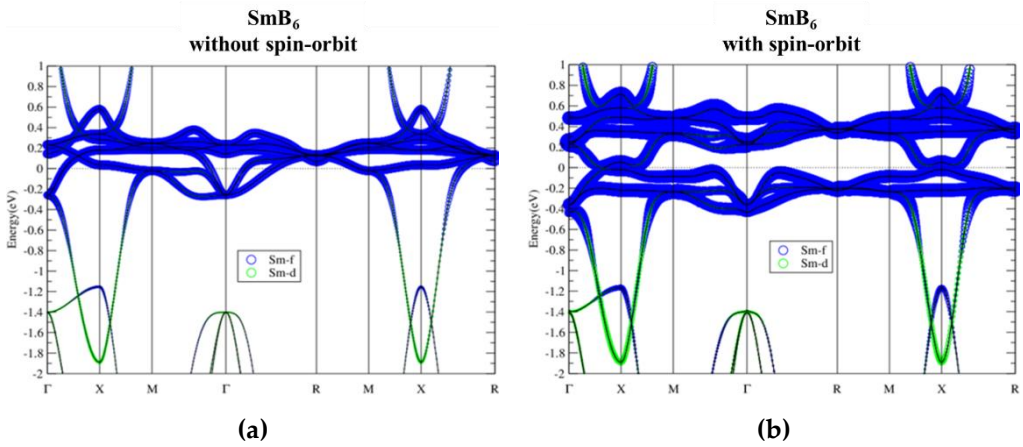

Figure 7. Band structures of SmB_6 without (**a**) and with (**b**) spin-orbit interaction projected by f and d electrons of Sm.

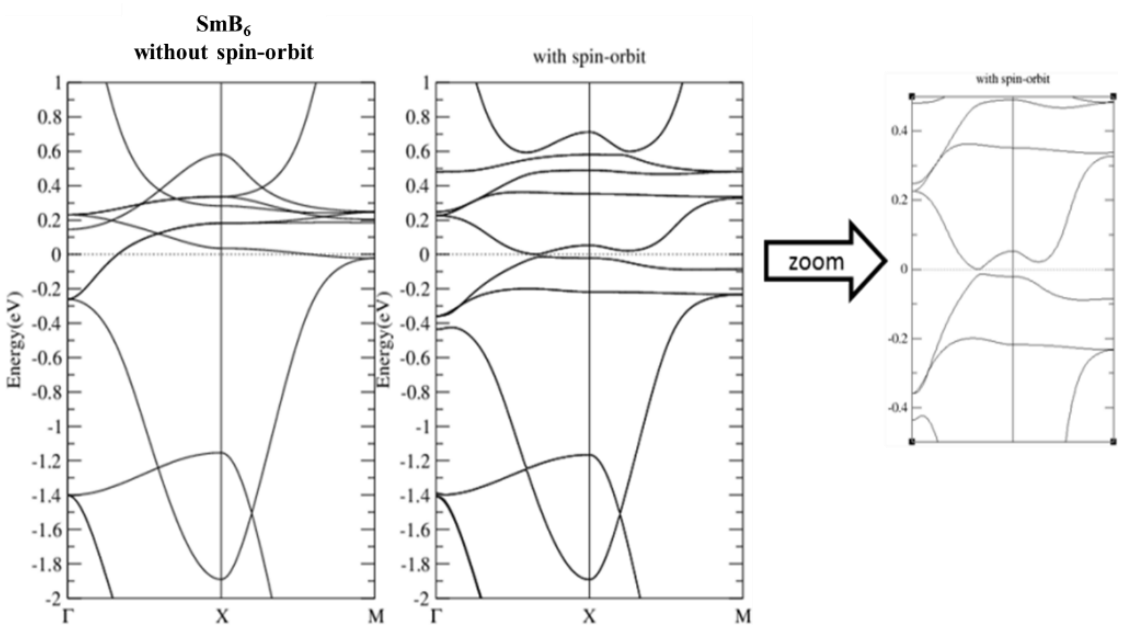

Figure 8. Band structure of SmB_6 without and with spin-orbit coupling. The right panel is the zoom-in view of the middle panel around E_f.

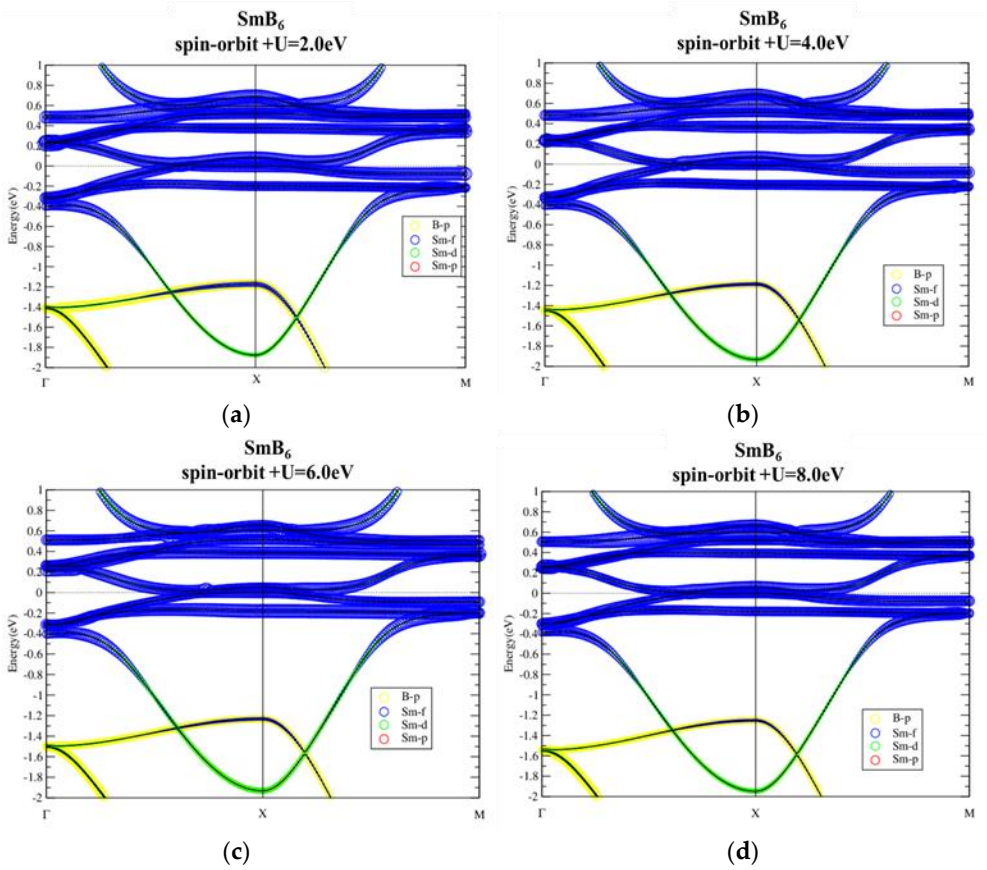

Figure 9. Band structures of SmB_6 with spin–orbit interaction using on-site U = 2.0, 4.0, 6.0, and 8.0 eV (**a**–**d**, respectively) projected by f and d electrons of Sm.

In comparison with the well-known topological Kondo insulator SmB_6, the overall band dispersion of PmB_6 as shown in Figure 10 is similar to those of SmB_6 (Figures 7–9). Since PmB_6 has one less valence electron than SmB_6, the Fermi level of PmB_6 is relatively lower than that of SmB_6. With SOI taken into consideration, PmB_6 opens up a continuous gap around Ef, as shown in Figure 10b,d. In addition, there is a band inversion around X point with B-p and Pm-d components exchanged near E_f. Therefore, PmB_6 can host topological nontrivial state, giving rise to the topological Kondo insulator similar to SmB_6. The electronic structure of PmB_6 around E_f is not sensitive to various U values, as shown in Figure 11. On-site U only affects the highest empty f-band without influencing the overall topological properties, indicating the topological phase is robust in PmB_6 against strong correlations.

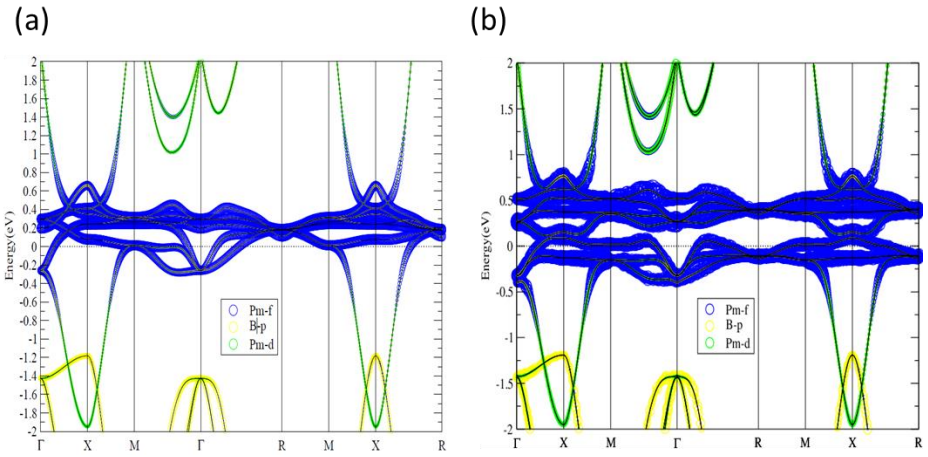

Figure 10. *Cont.*

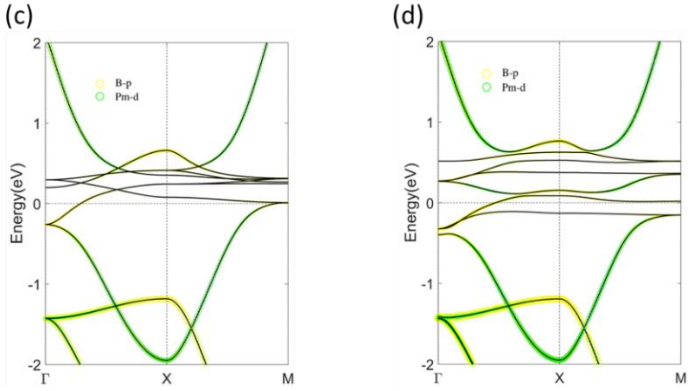

Figure 10. PBE band structure of PmB_6 without SOI (**a**) and with SOI (**b**). The size of blue, green and yellow circles show contributions from Pm-f, Pm-d and B-p orbitals, respectively. (**c**) Zoom-in of (**a**). (**d**) Zoom-in of (**b**). (**c**,**d**) demonstrate SOI-induced band inversion and gap opening.

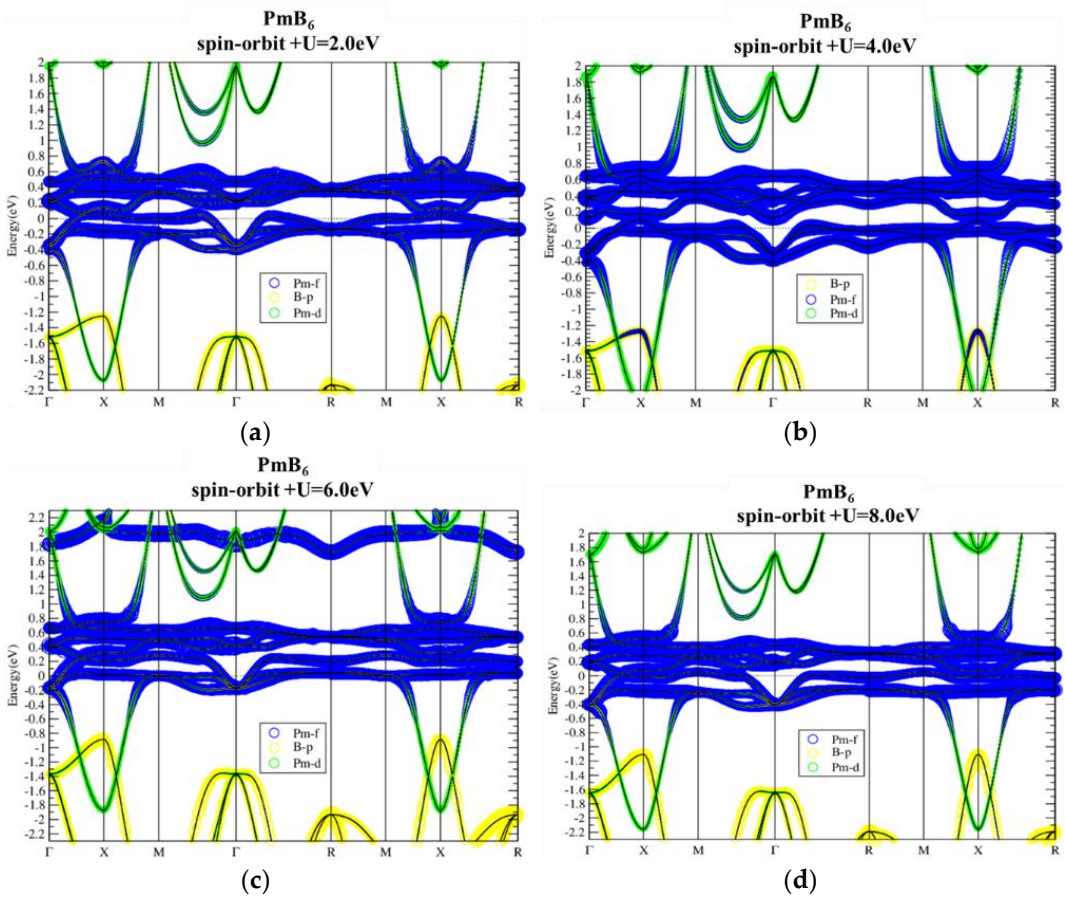

Figure 11. Band structures of PmB_6 with SOI and U = 2, 4, 6, 8 eV (**a**–**d**, respectively). As U is tuned larger, the highest f band is lifted but the band property is not changed near the Fermi level.

Band structures of NdB_6 as shown in Figure 12 also demonstrate topologically nontrivial phase. The SOI not only opens up a continuous energy gap around E_f but also gives rise to band inversion around X point. Similar to PmB_6, the electronic structure and topological behavior of NdB_6 near the Fermi level are insensitive to on-site U value, as can be seen in Figure 13. Only the highest unoccupied f band is noticeably modified by U, which is irrelevant to its topology. Consequently, NdB_6 is also a topological Kondo insulator.

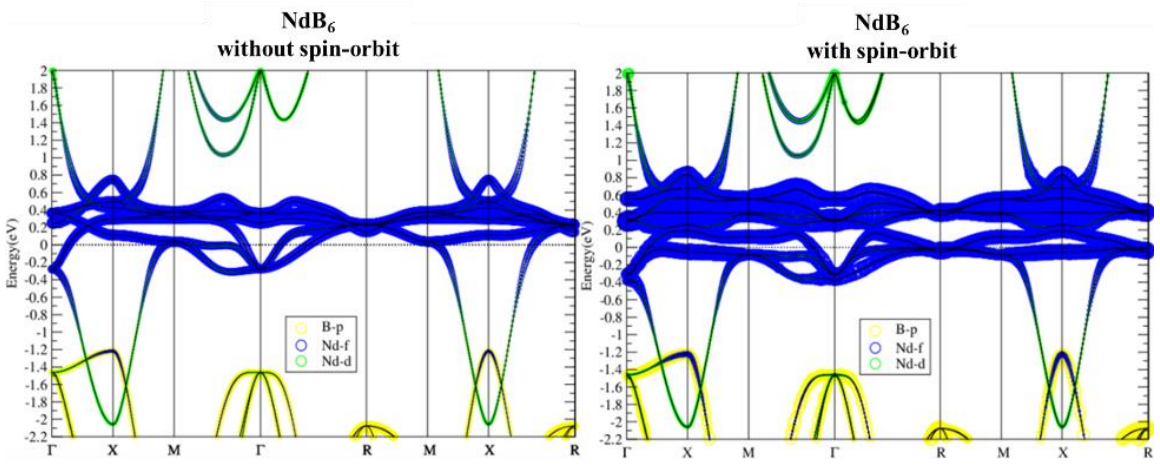

Figure 12. Band structures of NdB_6 without (**a**) and with (**b**) spin-orbit interaction.

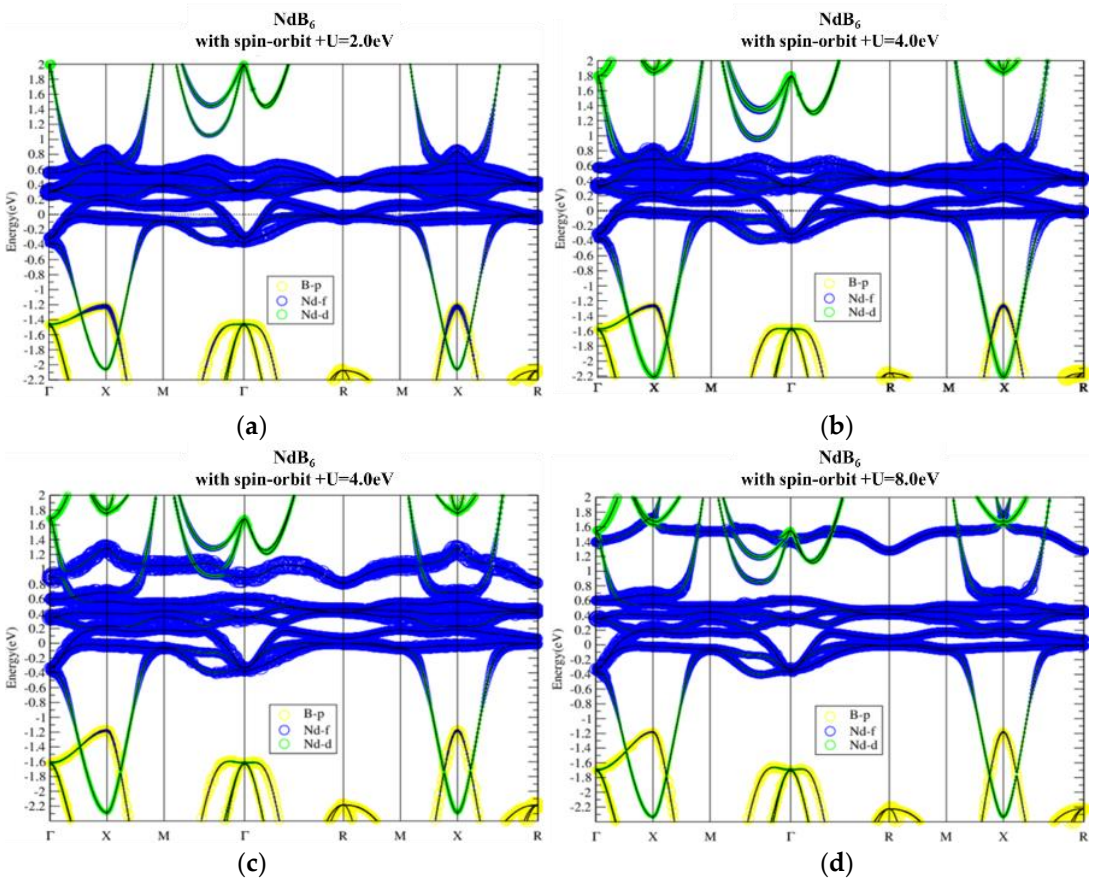

Figure 13. Band structures of NdB_6 with SOI using U = 2, 4, 6, and 8 eV (**a**–**d**, respectively). As U is tuned larger, the highest f band is lifted but the band property is not changed near the Fermi level.

Figure 14 shows PBE (U = 0 eV) band structures of EuB_6 without and with SOI as well as PBE + U band structures with U = 2 eV and 6 eV. As can be seen in Figure 14a, the f bands are located at E_f with a localized flat band character. In the periodic table, Eu is the neighbor of Sm with one more electron. The additional electron raises the Fermi level of EuB_6 near the half-filling metallic regime. When SOI is included, the f bands separate themselves into two groups with an SOI-induced continuous gap in between. Furthermore, band inversion emerges around the high symmetry point X. As a result,

EuB_6 exhibits nontrivial topological phase similar to SmB_6. The band structure of EuB_6 is not sensitive to U, as shown in Figure 14b–d, with U = 0–6 eV, leading EuB_6 to robust topological Kondo insulator against strong correlations.

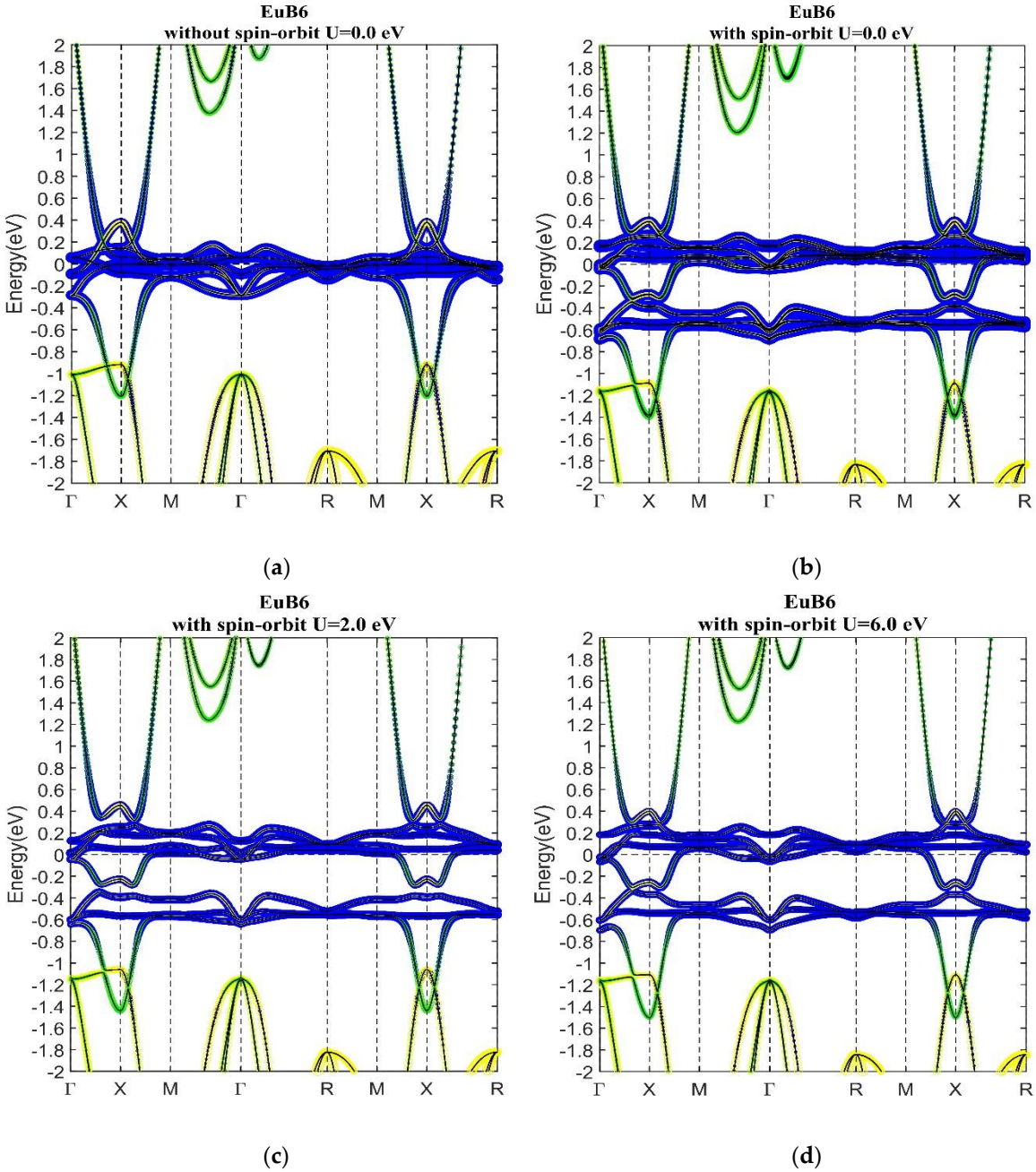

Figure 14. PBE band structure of EuB_6 without SOI (**a**) and with SOI (**b**). SOI opens up an energy gap around E_f and induces band inversion around X point. PBE + U band structure of EuB_6 with on-site U = 2.0 eV (**c**) and U = 6.0 eV (**d**). Similar to SmB_6, the Hubbard U does not change the band structure noticeably.

4. Conclusions

We have systematically analyzed the electronic structures of rare-earth hexaborides to investigate their topological properties and examine the robustness of the topological phase against strong correlations by varying the Coulomb repulsion U. SmB_6 is a topological Kondo insulator due to the hybridization gap, and it will not experience topological phase transition by tuning the Coulomb

interaction. YbB_6, which has a hybridization gap, on the contrary, will experience a topology phase transition from a topological Kondo insulator to a topological insulator, and finally become a trivial insulator. Our results of SmB_6 and YbB_6 are in good agreement with previous results [1]. Our study also shows that PmB_6, NdB_6, EuB_6 and SmB_6 exhibit SOI-induced continuous gaps with band inversion, revealing nontrivial topological properties. On the other hand, the weaker SOI in relatively lighter. Lanthanides La, Ce and Pr fail to open up a continuous gap in LaB_6, CeB_6 and PrB_6. Thus LaB_6, CeB_6 and PrB_6 are topologically trivial normal metals with correlated conduction electrons.

Author Contributions: S.-H.H. performed first-principles calculations and wrote the manuscript. H.-T.J. conducted the project and reviewed the manuscript. All authors have read and agreed to the published version of the manuscript.

Funding: This research received no external funding.

Acknowledgments: This work was funded by the Ministry of Science and Technology, Taiwan (grant number MOST 106-2112-M-007-012-MY3). The authors also thank support from NCHC, CINCNTU, AS-iMATE-109-13 and CQT-NTHU-MOE, Taiwan.

Conflicts of Interest: There are no conflicts of interest to declare.

References

1. Chang, T.-R.; Das, T.; Chen, P.-J.; Neupane, M.; Xu, S.-Y.; Hasan, M.Z.; Lin, H.; Jeng, H.-T.; Bansil, A. Two distinct topological phases in the mixed-valence compound YbB_6 and its differences from SmB_6. *Phys. Rev. B* **2015**, *91*, 155151. [CrossRef]
2. Weng, H.; Dai, X.; Fang, Z. Topological semimetals predicted from first-principles calculations. *J. Phys. Condens. Matter* **2016**, *28*, 303001. [CrossRef] [PubMed]
3. Kane, C.L.; Mele, E.J. Z_2 topological order and the quantum spin hall effect. *Phys. Rev. Lett.* **2005**, *95*, 146802. [CrossRef] [PubMed]
4. Hasan, M.Z.; Kane, C.L. Colloquim: Topological insulators. *Rev. Mod. Phys.* **2010**, *82*, 3045. [CrossRef]
5. Moore, J.E. The birth of topological insulators. *Nature* **2010**, *464*, 194–198. [CrossRef]
6. Qi, X.-L.; Zhang, S.-C. Topological insulators and superconductors. *Rev. Mod. Phys.* **2011**, *83*, 1057–1110. [CrossRef]
7. Fu, L.; Kane, C.L. Topological insulators with inversion symmetry. *Phys. Rev. B* **2007**, *76*, 045302. [CrossRef]
8. Schell, G.; Winter, H.; Rietschel, H.; Gompf, F. Electronic structure and superconductivity in metal hexaborides. *Phys. Rev. B* **1982**, *25*, 1589–1599. [CrossRef]
9. Demishev, S.V.; Semeno, A.; Bogach, A.; Paderno, Y.; Shitsevalova, N.; Sluchanko, N. Antiferro-quadrupole resonance in CeB6. *Phys. B Condens. Matter* **2006**, *378–380*, 602–603. [CrossRef]
10. Barman, C.K.; Singh, P.; Johnson, D.D.; Alam, A. Revealing the nature of antiferroquadrupolar ordering in cerium hexaboride: CeB6. *Phys. Rev. Lett.* **2019**, *122*, 076401. [CrossRef]
11. Morin, P.; Kunii, S.; Kasuya, T. Quadrupolar properties and magnetic phase diagrams in PrB6 hexaboride compound. *J. Magn. Magn. Mater.* **1991**, *96*, 145–154. [CrossRef]
12. Matthias, B.T.; Geballe, T.H.; Andres, K.; Corenzwit, E.; Hull, G.W.; Maita, J.P. Superconductivity and antiferromagnetism in boron-rich lattices. *Science* **1968**, *159*, 530. [CrossRef] [PubMed]
13. Wolgast, S.; Kurdak, Ç.; Sun, K.; Allen, J.W.; Kim, D.-J.; Fisk, Z. Low-temperature surface conduction in the Kondo insulator SmB_6. *Phys. Rev. B* **2013**, *88*, 180405. [CrossRef]
14. Zhang, X.; Butch, N.; Syers, P.; Ziemak, S.; Greene, R.L.; Paglione, J. Hybridization, inter-ion correlation, and surface states in the kondo insulator SmB_6. *Phys. Rev. X* **2013**, *3*, 011011. [CrossRef]
15. Booth, C.H.; Sarrao, J.L.; Hundley, M.F.; Cornelius, A.L.; Kwei, G.H.; Bianchi, A.; Fisk, Z.; Lawrence, J.M. Local and average crystal structure and displacements of $La^{11}B_6$ and EuB_6 as a function of temperature. *Phys. Rev. B* **2001**, *63*, 224302. [CrossRef]
16. Pickard, C.J.; Winkler, B.; Chen, R.K.; Payne, M.C.; Lee, M.H.; Lin, J.S.; White, J.A.; Milman, V.; Vanderbilt, D. Structural properties of lanthanide and actinide compounds within the plane wave pseudopotential approach. *Phys. Rev. Lett.* **2000**, *85*, 5122. [CrossRef] [PubMed]
17. Degiorgi, L.; Felder, E.; Ott, H.R.; Sarrao, J.L.; Fisk, Z. Low-temperature anomalies and ferromagnetism of EuB_6. *Phys. Rev. Lett.* **1997**, *79*, 5134–5137. [CrossRef]

18. Süllow, S.; Prasad, I.; Aronson, M.C.; Bogdanovich, S.; Sarrao, J.L.; Fisk, Z. Metallization and magnetic order inEuB6. *Phys. Rev. B* **2000**, *62*, 11626–11632. [CrossRef]
19. Kunii, S.; Takeuchi, K.; Oguro, I.; Sugiyama, K.; Ohya, A.; Yamada, M.; Koyoshi, Y.; Date, M.; Kasuya, T. Electronic and magnetic properties of GdB_6. *J. Magn. Magn. Mater.* **1985**, *52*, 275–278. [CrossRef]
20. Weng, H.; Zhao, J.; Wang, Z.; Fang, Z.; Dai, X. Topological crystalline kondo insulator in mixed valence ytterbium borides. *Phys. Rev. Lett.* **2014**, *112*, 016403. [CrossRef]
21. Xia, M.; Jiang, J.; Ye, Z.R.; Wang, Y.H.; Zhang, Y.; Chen, S.D.; Niu, X.H.; Xu, D.F.; Chen, F.; Chen, X.H.; et al. Angle-resolved photoemission spectroscopy study on the surface states of the correlated topological insulator YbB_6. *Sci. Rep.* **2014**, *4*, srep05999. [CrossRef] [PubMed]
22. Walker, H.C.; McEwen, K.A.; McMorrow, D.F.; Bleckmann, M.; Park, J.-G.; Lee, S.; Iga, F.; Mannix, D. X-ray resonant scattering study of the structural and magnetic transitions in PrB_6. *Phys. Rev. B* **2009**, *79*, 054402. [CrossRef]
23. Allen, A. *Phase Diagrams 6-V: Materials Science and Technology*; Elsevier: Amsterdam, The Netherlands, 2012.
24. Kresse, G.; Hafner, J. Ab initio molecular-dynamics simulation of the liquid-metal-amorphous-semiconductor transition in germanium. *Phys. Rev. B* **1994**, *49*, 14251. [CrossRef] [PubMed]
25. Kresse, G.; Furthmüller, J. Efficient iterative schemes for ab initio total-energy calculations using a plane-wave basis set. *Phys. Rev. B* **1996**, *54*, 11169–11186. [CrossRef]
26. Blöchl, P.E. Projector augmented-wave method. *Phys. Rev. B* **1994**, *50*, 17953. [CrossRef]
27. Perdew, J.P.; Burke, K.; Ernzerhof, M. Generalized gradient approximation made simple. *Phys. Rev. Lett.* **1996**, *77*, 3865–3868. [CrossRef] [PubMed]
28. MacKinnon, I.D.; Alarco, J.A.; Talbot, P.C. Metal hexaborides with Sc, Ti or Mn. *Model. Numer. Simul. Mater. Sci.* **2013**, *3*, 158–169. [CrossRef]
29. Blomberg, M.; Merisalo, M.; Korsukova, M.; Gurin, V. Single-crystal X-ray diffraction study of NdB_6, EuB_6 and YbB_6. *J. Alloys Compd.* **1995**, *217*, 123–127. [CrossRef]